PERGAMON

Journal of Structural Geology 22 (2000) 1125–1139

JOURNAL OF STRUCTURAL GEOLOGY

www.elsevier.nl/locate/jstrugeo

Dextral transpression in Late Cretaceous continental collision, Sanandaj–Sirjan Zone, western Iran

Mohammad Mohajjel [1], Christopher L. Fergusson*

School of Geosciences, University of Wollongong, Wollongong, New South Wales 2522, Australia

Received 18 May 1998; accepted 15 March 2000

Abstract

The Sanandaj–Sirjan Zone of western Iran is a metamorphic belt (greenschist–amphibolite) that was uplifted during Late Cretaceous continental collision between the Afro-Arabian continent and the Iranian microcontinent. In the June area, 300 km southwest of Tehran, the Late Palaeozoic–Mesozoic succession was affected by two major episodes of deformation. The first deformation formed tight folds and axial plane schistosity. These are strongly overprinted by second deformation structures that formed during Late Cretaceous continental collision under dextral transpression. The convergence has a low obliquity and has significant deformation partitioning into two domains. (1) A widespread schist and marble domain with intensely folded and foliated rocks that are cut by thrusts and have an overall south-southwest vergence. (2) A domain with wide zones of mylonitic granite, amphibolite and less common calcite mylonite that are affected by a foliation with the same orientation as in rocks of the schist and marble domain. Rocks of this domain also contain an intense sub-horizontal stretching lineation and abundant shear-sense criteria indicating dextral shear. This contrasts with many zones of transpression where strike-slip shearing is taken up along discrete faults. A syn-D_2 pluton (the Galeh–Doz pluton) has a major S-shaped bend within it, imparted during the dextral transpression.

1. Introduction

The Zagros Orogen formed by continental collision between the Afro-Arabian continent and the Iranian microcontinent in Late Cretaceous to Tertiary time (Berberian and King, 1981). Widespread thrusting has been attributed to the collision in the Sanandaj–Sirjan Zone (Fig. 1; Alavi, 1994). In addition to thrust faults, ductile structures, including tight-isoclinal folds and associated foliations and lineations abound in the metamorphosed Late Palaeozoic and Mesozoic succession and plutonic rocks developed in the Dorud–Azna region in the central part of the Sanandaj–Sirjan Zone (Fig. 1). This paper is concerned with the documentation of deformation produced before and during the continental collision in the northern Dorud–Azna region (June area of 350 km^2) located 300 km southwest of Tehran (Fig. 1). Our aims are to (1) document the structure of the June area, (2) examine the role of dextral transpression associated with the dominant second deformation, and (3) discuss the probable relationship between intrusion of an S-shaped granitic pluton (the Galeh–Doz pluton) and the transpressional regime.

In common with many other orogenic belts deformation in the Zagros Orogen reflects transpression rather than normal shortening across the orogen (e.g. Dewey et al., 1998). Many zones with transpression have non-coaxial deformation developed along weak narrow faults (e.g. Teyssier et al., 1995) whereas in the study area, the strike-slip component of the transpression has occurred over wide zones of deformed rock. Another issue has been the difficulty in evaluating the relative competency of granitic rocks found in zones of

* Corresponding author.
E-mail address: Chris_Fergusson@uow.edu.au (C.L. Fergusson).
[1] Present address: Department of Geology, Tarbiat Modarres University, P.O. Box 14155-4838, Tehran, Iran

0191-8141/00/$ - see front matter
PII: S0191-8141(00)00023-7

non-coaxial deformation which normally contain less competent units (e.g. Ridley, 1986).

2. Geological background

The Zagros Orogen of western Iran consists of four parallel tectonic zones from the northeast to southwest (Fig. 1): (1) the Urumieh–Dokhtar Magmatic Arc, (2) the Sanandaj–Sirjan Zone, (3) the Zagros Fold–Thrust Belt, and (4) the Mesopotamian–Persian Gulf foreland basin (Berberian and King, 1981; Alavi, 1994). The Sanandaj–Sirjan Zone extends for 1500 km along strike from northwest (Sanandaj) to southeast (Sirjan) in the western part of Iran and has a width of 150–200 km (Fig. 1). It consists of Palaeozoic strata formed in an epicratonic setting that were subsequently overlain by a volcanic and sedimentary succession deposited during the Triassic opening of Neo-Tethys (e.g. Sengör et al., 1988). The orogenic belt is the result of closure of Neo-Tethys by consumption of oceanic crust at a northeast-dipping subduction zone below central Iran and subsequent Cretaceous continental collision between the Afro-Arabian and Iranian continental fragments (e.g. Alavi, 1994).

The study area contains a late Palaeozoic to Mesozoic succession dominated by metacarbonate, schist and amphibolite and intruded by deformed granite (Figs. 2 and 3; Mohajjel, 1997). Four stratigraphic units are mapped including the Permian Kuh-e-June Metacarbonate, the Middle–Late Triassic June Complex (subdivided into three units), the Late Triassic–Jurassic Hamadan Phyllite and Late Jurassic–Early Cretaceous andesitic lavas and pyroclastic rocks that are conformably overlain by Aptian–Albian limestone (Figs. 2 and 3).

The metasedimentary and metavolcanic rocks were intruded by the Galeh–Doz pluton, a member of a suite of Late Cretaceous to Palaeocene plutons in the northwestern Sanandaj–Sirjan Zone (Mohajjel, 1997). The older deformed members of this suite have K–Ar and Rb–Sr ages of 120–70 Ma whereas the undeformed members have ages of 70–50 Ma (Valizadeh, 1992; Masoudy, 1997). The main exposure of the Galeh–Doz pluton is in the eastern part of the study area with a long sill-like extension to the west-northwest and another sheet-like exposure around Shur-Shur village in the central part of the study area. The Galeh–Doz pluton consists of microcline, plagioclase, biotite, quartz and muscovite with feldspar augen.

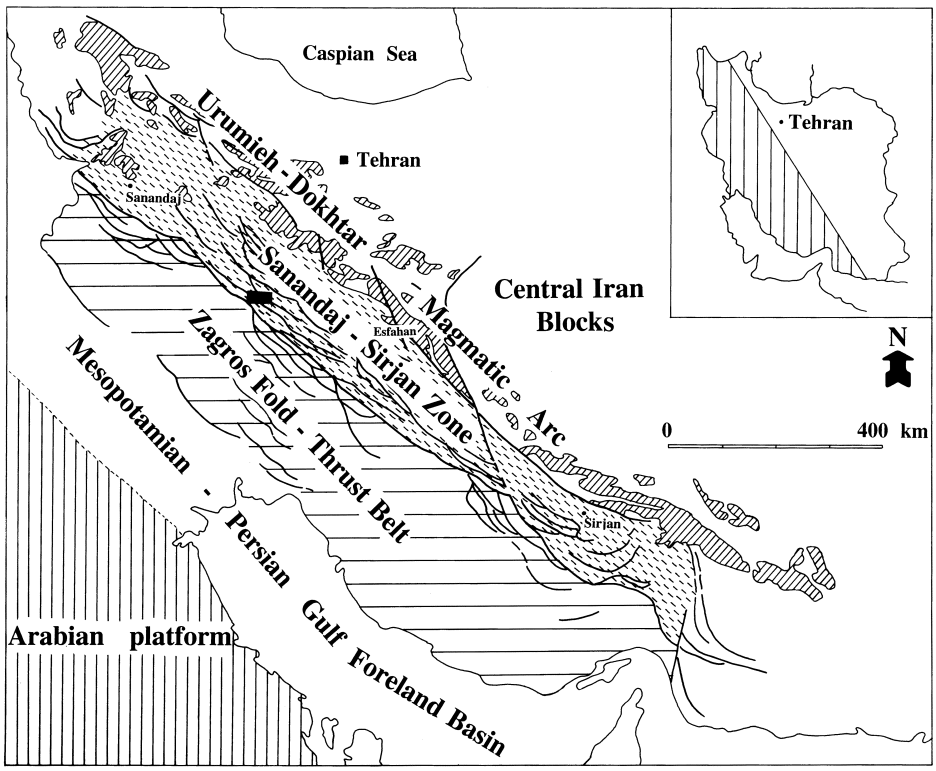

Fig. 1. Tectonic zones of the Zagros Orogen in western Iran (after Alavi, 1994) and location of the study area (black inset) in the Dorud–Azna region of the Sanandaj–Sirjan Zone.

Undeformed dolerite of presumed Tertiary age has intruded and post-dates structures in the study area (Fig. 3).

3. D_1 deformation

D_1 structures include mesoscopic folds, axial planar schistosity, and macroscopic folds. They are well documented in quartzite, schist and marble of the greenschist metamorphic rocks of the June Complex in the Papion and Bavaki areas (Fig. 3) but have been only rarely found elsewhere in the study area. Mesoscopic folds (F_1) are commonly tight to isoclinal (Fig. 4a) but are locally tighter than isoclinal (mushroom-shaped). Axial planes dip moderately to steeply (50–80°) to the east with variable strikes due to later folding (Fig. 5). F_1 plunge at 40–60° to the northeast (Fig. 5). Boudinage is developed along the limbs of F_1 folds.

S_1 is developed axial planar to F_1 and on the limbs of folds is commonly parallel to bedding (S_0). It is well developed in schist and thin-layered marble and also occurs in metadolomite and quartzite but is only rarely recognised in phyllite. S_1 is a metamorphic structure as shown by syntectonic mineral growth. In schist, S_1 is defined by alignment of muscovite and biotite flakes whereas in quartzite S_1 is defined by elongate recrystallised detrital quartz grains with internal polygonal mosaic texture. In phyllite, S_1 is transposed by S_2, but locally at a microscopic scale S_1 is preserved in hinge areas of F_2 microfolds (Fig. 4b). In amphibolite, S_1 is defined by segregation layering with feldspar-rich and amphibole-rich bands. These rocks contain relics of aligned metamorphic brown hornblende that are retrogressed to actinolite.

Macroscopic F_1 structures in the study area are isoclinal folds with attenuated long limbs and elongate angular hinges. Around Papion village, a macroscopic F_1 fold couple with a west-northwest-trending elongate hinge zone is exposed (Figs. 3, 6 and 7). This structure is refolded by F_2 with west-northwest-trending axial surfaces (see below). Northwest of Bavaki, bedding orientations and stratigraphic units define a complex set of interference fold patterns formed by several map-scale northerly trending F_1 anticlines that are refolded by northwest-trending F_2 folds (see Section 4.2; Fig. 3). Cross bedding, preserved in quartzite of the lower unit of the June Complex, indicates younging directions that define the cores of these F_1 folds.

4. D_2 deformation

This deformation produced the dominant structures

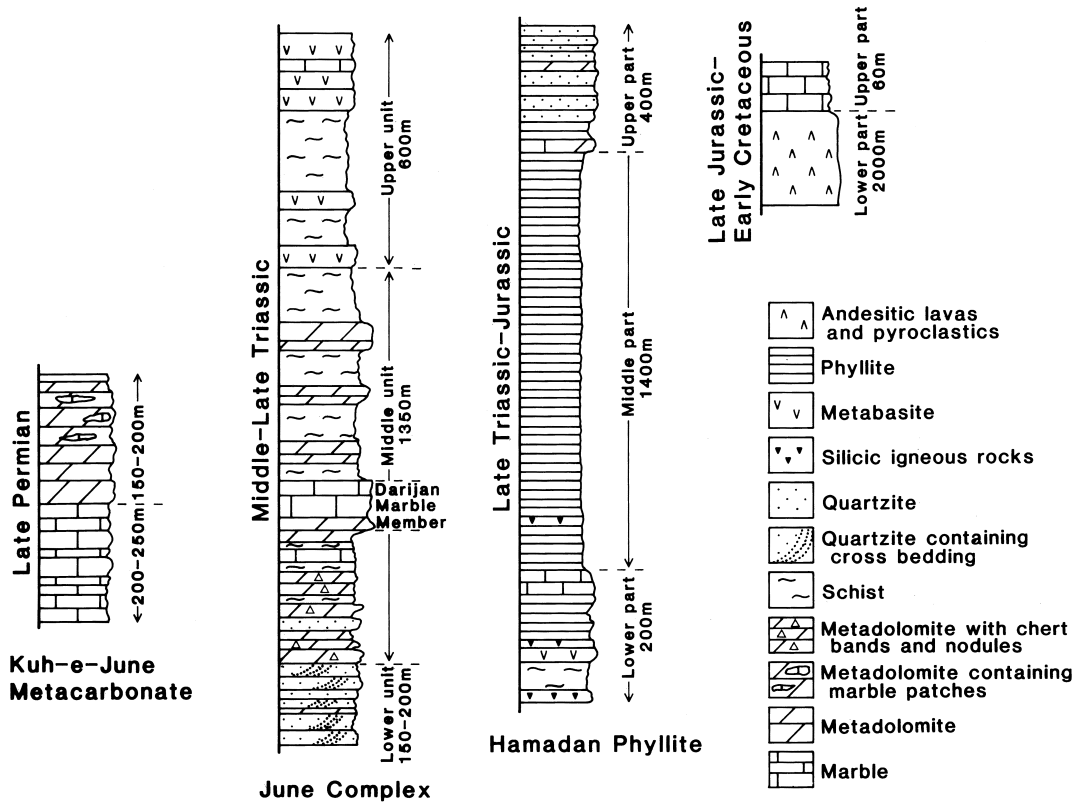

Fig. 2. Stratigraphic columns of the June area (not to scale) with approximate stratigraphic thicknesses of units.

in the study area and developed by intense folding of S_0 and S_1. Folds (F_2) and the axial plane schistosity (S_2) are the most abundant structures formed during D_2. Widely developed mylonitic fabrics in crystalline rocks were formed during D_2.

4.1. Mesoscopic structures

F_2 folds are abundant in thin-layered marble and less common in thick-bedded and massive metadolomite, quartzite and phyllite. They are tight to isoclinal with angular hinges in schist and calcschist whereas angular to rounded hinges occur in quartzite and metadolomite (e.g. Fig. 8a). Some F_2 folds are intrafolial and are bounded on either side by planar surfaces (lithological layering parallel to S_2). Axial planes of these folds have moderate to steep dips to the northeast with axes plunging moderately to the east (Fig. 9). Low amplitude folds with parallel geometry occur in competent quartzite and dolomite, whereas folds with high amplitudes and short wavelengths occur in schist and calcschist (Fig. 8a).

An S_2 axial plane schistosity is well developed and has an almost constant west-northwest strike and steep dip to the north-northeast throughout the study area (Fig. 9c). S_2 is defined by the alignment of white mica and chlorite in schist, aligned actinolite in metabasic rocks and aligned sericite and chlorite in phyllite. In quartzite, S_2 is defined by alignment of ellipsoidal quartz grains with mica flakes. S_2 is generally parallel to the compositional layering. On F_2 limbs, S_0 and S_1 are commonly transposed parallel to S_2 except in F_2 hinges where lithological layering is trending north–south. At these localities, compositional layering is sub-parallel to S_1 and is cut by the S_2 foliation that has crenulation morphology (Fig. 4b). A widespread intersection lineation (L_2^1) between S_1 and S_2 is developed sub-parallel to F_2 fold axes in schist (Fig. 9b).

Abundant boudinage and pinch-and-swell structures are associated with F_2. Competent metadolomite and quartzite layers in incompetent marble and schist and competent metabasite in incompetent marble contain boudinage and pinch-and-swell structures (Fig. 8b). Chert bands in metadolomite and marble are also bou-

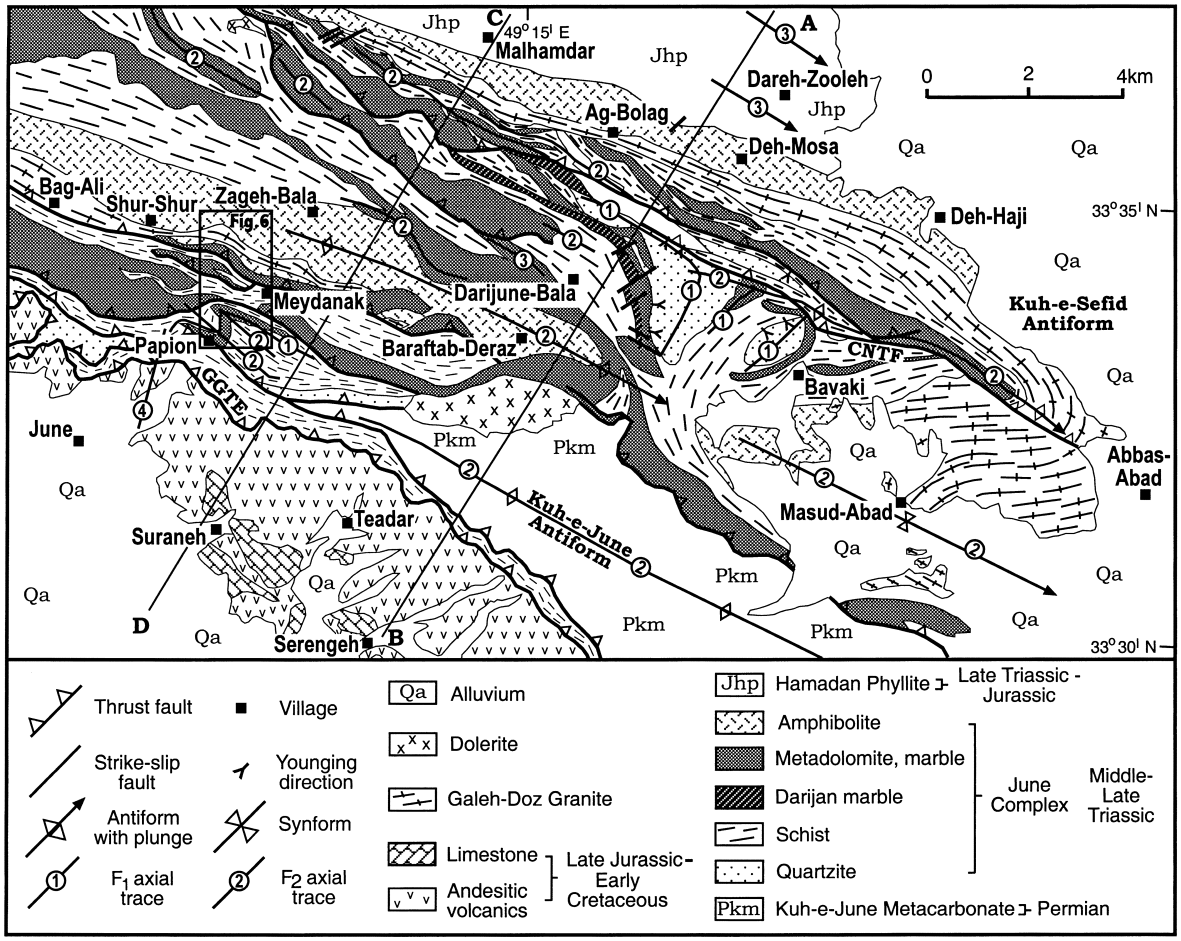

Fig. 3. Major structures and units in the June area. Abbreviations: GGTF, Galeh–Gurchak thrust fault, CNTF, Cheshmeh–Narges thrust fault. Map-scale folds are labelled 1, 2, 3, and 4 for F_1, F_2, F_3 and F_4, respectively.

dinaged. First generation boudins were refolded and the shape of boudins and pinch-and-swell structures were modified during D_2.

The first fold axial surfaces and hinges are strongly folded by the new generation folds (F_2) producing mesoscopic interference patterns. They are well exposed in the north-trending limb of the Papion parasitic F_2 folds (Fig. 4c). Two-dimensional interference patterns range between types 2 and 3, patterns H and I of Ramsay (1967, p. 531).

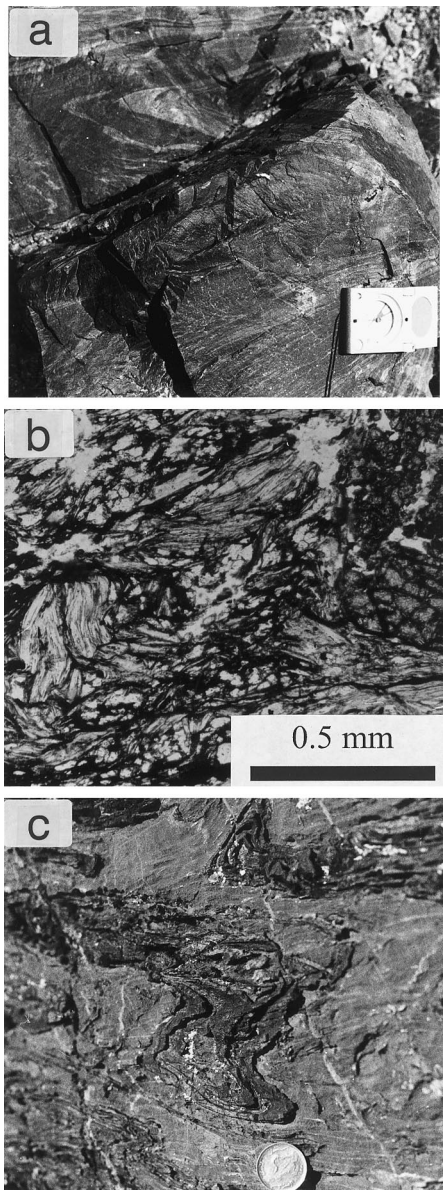

Fig. 4. (a) Tight F_1 fold in fine-grained quartzite interbedded with thin-layered and partly boudinaged metadolomite, 3 km east of Darijune–Bala. Compass is 12 cm in length. (b) Relic S_1 preserved amongst well-developed S_2. Garnet–muscovite schist with S_2 wrapped around part of a sub-idiomorphic syn-D_2 garnet porphyroblast (right side of photograph), 2 km northeast of Teadar, June Complex, middle unit, sample number 847 (plane polarised light). Samples are housed in the School of Geosciences, University of Wollongong reference collection. (c) Type 3 interference patterns produced by coaxial superimposition of F_2 on F_1, 200 m east of Papion, coin is 16 mm in diameter.

4.2. Macroscopic folds

Several map-scale, isoclinal, high-amplitude, west-northwest-trending F_2 antiforms dominate the study area (Fig. 3). Lithological layering and axial plane schistosity associated with these folds dip steeply towards the north-northeast and the axes plunge moderately to the east. These structures are overturned with vergence to the southwest. Southwestern limbs are attenuated and several north-northeast dipping thrust faults are developed (Fig. 10). The succession in the main F_2 antiform around Zageh–Bala and Baraftab–Deraz (Fig. 3) is younging into the core of the structure with the middle unit of the June Complex (metadolomite and schist) on the limbs and the upper unit of the June Complex in the core (amphibolite). Thus the younging direction contained within the axial plane of the main F_2 antiform is downward (i.e. the fold is downward facing), although local way-up structures can only be identified in the lower unit of the June Complex (cross-bedded quartzite) in the cores of F_1 anticlines. This fold therefore has affected the lower overturned limb of a major F_1 anticline (Fig. 3).

Macroscopic interference patterns occur at the hinge area of the map-scale F_2 folds 3 km northeast of Baraftab–Deraz (Fig. 3). Quartzite in the core of the map-scale F_1 fold is exposed in a boomerang-shaped interference pattern (type 2 of Ramsay, 1967). Other macroscopic interference patterns in the Bavaki area were produced by macroscopic F_2 superimposed on F_1 and form crescent-type interference patterns.

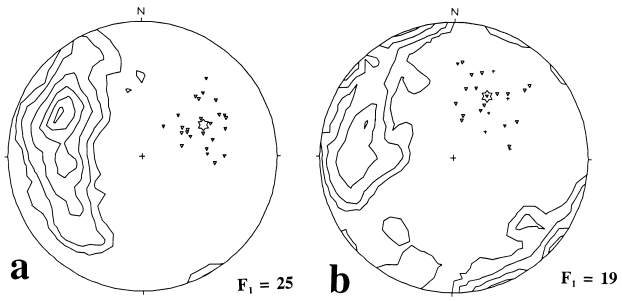

Fig. 5. (a) Lower-hemisphere equal-area stereographic projection of D_1 structural elements measured on the Papion fold. AS1 and S_1 poles (92) are contoured at 1, 2, 4, 6, 8, and 10% per 1% area. F_1 = triangles and average is shown by star is 48°/063°. (b) Lower-hemisphere equal-area stereographic projection of D_1 structural elements measured in the Bavaki area, eastern half of the study area. AS1, S_1, and S_0 poles (130) are contoured at 1, 2, 4, and 6% per 1% area. F_1 = triangles and average is shown by star is 47°/028°, L_1 = crosses.

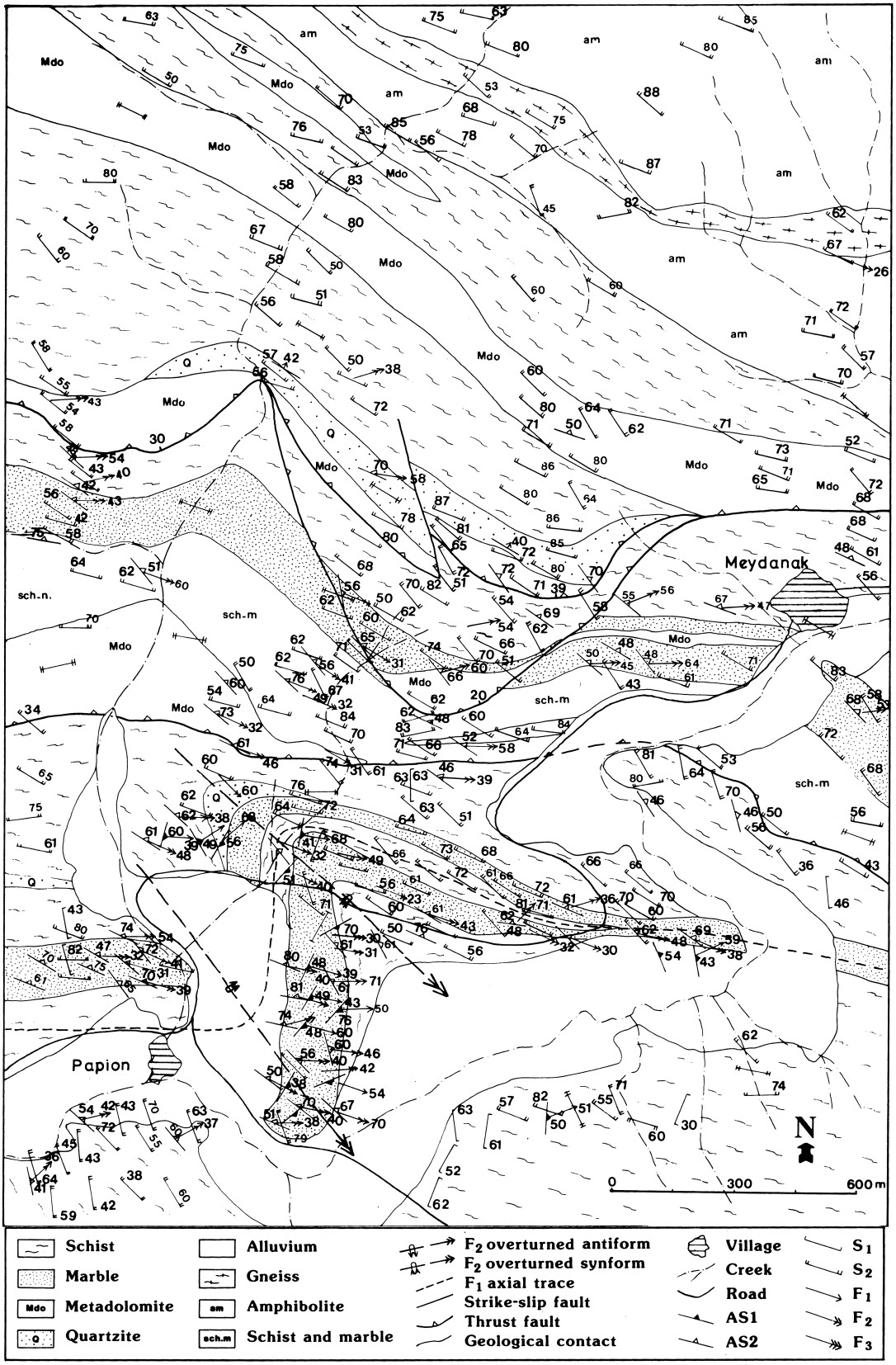

Fig. 6. Structure map of the Papion–Meydanak district.

4.3. Faults

Faulting throughout the study area has contributed to the complex nature of the outcrop pattern with dominant west-northwest-trending and north-northeast-dipping thrust faults (Fig. 3). Thrust faults are mostly developed along the overturned limbs of F_2 folds. In the southwestern part of the mapped area, along the west-northwest-trending overturned limb of the map-scale F_2 antiform, thrust faults are at low angles or are even horizontal. Younger rocks faulted over older rocks (e.g. Galeh–Gurchak thrusts, Fig. 3), *S–C* fabrics in fault zones, and striation orientations show thrust displacement (Fig. 11, see also Mohajjel, 1997).

The Permian Kuh-e-June Metacarbonate is in fault contact with the overlying Middle–Late Triassic June Complex to the north of the Kuh-e-June antiform (Fig. 3). In contrast to other faults in the study region that are thrusts, this fault juxtaposes stratigraphically younger rocks in the hanging wall against older rocks in the footwall. This pattern is anomalous for the D_2 deformation as F_2 folds have a consistent southwest vergence and associated thrust faults are developed along the overturned F_2 limbs. One possibility is that this fault formed prior to D_2, perhaps during an earlier phase of extension, and was reactivated as a thrust during D_2 and D_1.

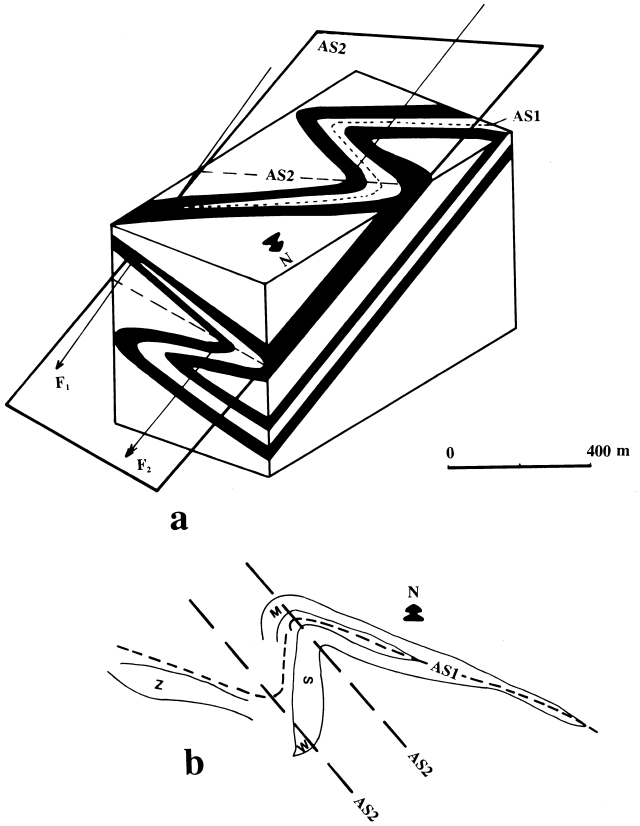

Fig. 7. (a) Schematic block diagram showing the Papion F_1 fold refolded by F_2. (b) The isoclinal Papion F_1 fold is folded by S-type F_2 folds [same scale as for (a)]. Outcrop trace of folds from 1:20 000 scale air photo and location of S-, Z- and M-type mesoscopic F_2 in the macroscopic S-type folds.

5. Structure of the mylonitic rocks

Four major types of mylonitic rocks occur in the study area: (1) mylonitic granite, (2) mylonitic amphibolite, (3) calcite mylonite, and (4) mylonitic fine-grained silicic igneous rocks. The main foliation in these mylonitic rocks is subparallel to S_2 elsewhere and contains a well-developed, gentle to subhorizontal stretching lineation not found in the marble and schist domain.

5.1. Mylonitic granite

The mylonitic granite has a compositional layering and foliation parallel to S_2 formed by interbanded quartzo-feldspathic and mafic layers (Fig. 12). Biotite sub-parallel to quartz ribbons and feldspar define the foliation. Quartz occurs in ribbons as polygonised

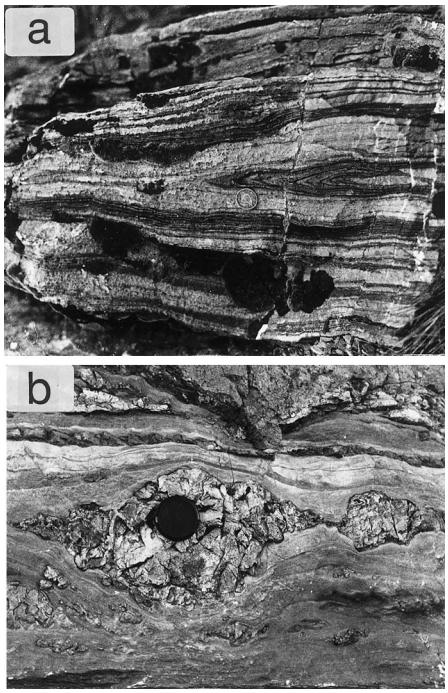

Fig. 8. (a) Isoclinal F_2 fold in marble, 1 km northeast of Papion. Coin is 16 mm across. (b) Boudins in competent metadolomite parallel to S_2. Note the asymmetric boudin in the centre of the photograph and also the much smaller asymmetric boudins in thin-layered metadolomite above the lens cap which are displaced dextrally along small shear fractures. The shear fractures cut S_2, lithological layering and boudinage, 600 m southeast of Shur-Shur. Lens cap is 5.5 cm in diameter.

grains and in pressure shadows at the end of feldspar porphyroclasts. Quartz porphyroclasts contain subgrains with sutured boundaries. Fine quartz grains occur at the boundaries of larger quartz grains and at the borders of quartz ribbons. Undulatory extinction is developed in the quartz ribbons. Elongate feldspar grains define the foliation and are wrapped around by quartz ribbons.

The steeply dipping mylonitic foliation has a sigmoidal trend in the central portion of the Galeh–Doz pluton (Fig. 3). From north to south, the S_2 mylonitic foliation is folded around an F_2 antiform and swings from a northwest to an easterly strike and farther south strikes northwest–southeast (Fig. 3). The west-northwest-trending extension of the Galeh–Doz pluton, the Shur-Shur pluton and other exposures of the deformed granite also contain the pervasive west-northwest-trending mylonitic foliation (S_2). This foliation is vertical or dipping steeply to the northeast.

In the Galeh–Doz pluton and other mylonitic granitic rocks, a strong sub-horizontal to gently plunging stretching lineation (L_m) is present within S_2 (Fig. 12). In the main mass of the pluton, this lineation plunges 20–30° to the northeast and in the west-northwest extension of the Galeh–Doz pluton and the Shur-Shur pluton it is subhorizontal or plunging gently to both the northwest and southeast (Fig. 12). The stretching lineation is contained within the strong mylonitic foliation (S_2) and is defined by elongate and extended biotite, quartz ribbons and feldspar porphyroclasts. In the northwestern extension of the Galeh–Doz pluton, cylindrical rods consisting of tourmaline also show stretching. Pinch-and-swell structures also occur in the mylonitic granite; the extension direction indicated by these structures is sub-parallel to the stretching lineation (L_m) in S_2.

Dextral shear deformation is indicated by porphyroclast asymmetries. Asymmetric augen structures (σ-

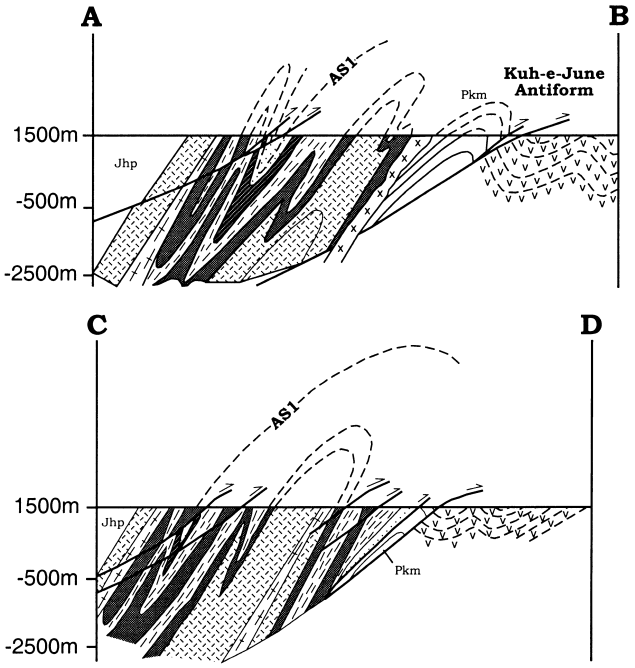

Fig. 10. Cross-sections AB and CD (note that horizontal scale = vertical scale). See Fig. 3 for location and key to symbols.

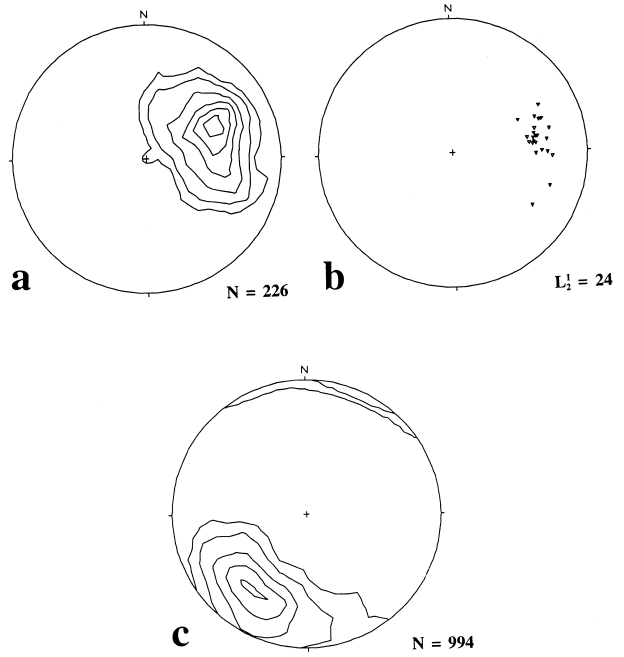

Fig. 9. Lower-hemisphere equal-area stereographic projections of D_2 structural data measured in the study area. (a) F_2 is contoured at 1, 2, 4, 6 and 8% per 1% area. The mean orientation is 62°/067°. (b) Intersection lineation (S_2–S_1) in Papion parasitic folds. The mean orientation is 47°/095°. (c) AS2 and S_2 are contoured at 1, 2, 4, 6, 8 and 10% per 1% area. The mean orientation is 64°/034°.

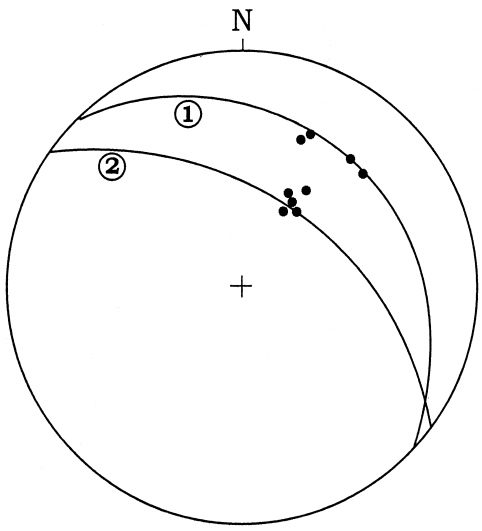

Fig. 11. Lower-hemisphere equal-area stereographic projection of striations (dots) along the Galeh–Gurchak thrust fault (1) and Cheshmeh–Narges thrust fault (2).

type) are defined in horizontal exposures. Feldspar augen occur in a fine-grained matrix and have asymmetric tails of fine-grained recrystallised material of the same composition as the porphyroclast (cf. White et al., 1980). Tails are extended along the foliation plane and are asymmetrically distributed around the porphyroclasts.

5.2. Amphibolite mylonite

West-northwest-trending amphibolite mylonite is located in the core of the map-scale F_2 antiform and in the northeast of the study area (Fig. 3). A metamorphic segregation layering composed of plagioclase-rich and amphibole-rich layers is present in the amphibolites. The segregation layering in the amphibolite is tightly to isoclinally folded with axial planes of the folds parallel to the gross mylonitic foliation (S_2) with a west-northwest orientation steeply dipping to the north-northeast.

The stretching lineation (L_m) in the mylonitic S_2 is defined by elongate plagioclase and amphibole and is sub-horizontal or plunges gently to the northwest or southeast (Fig. 12). Also, subhorizontal mechanical striations occur in the mylonitic foliation indicating strike-slip displacement (cf. Berthe et al., 1979). Pinch-and-swell structures along S_2 indicate extension subparallel to the stretching lineation.

Shear-sense indicators consistently indicate a dextral sense. Composite *C*- and *S*-surfaces (Berthe et al., 1979) are developed in amphibolite mylonite along with mica-fish structure (type-II *S*–*C* mylonite of Lister and Snoke, 1984) defined by amphibole. The *S*-planes are indicated by aligned hornblende with tails extended along the *C*-planes. They are linked by thin trails of amphibole fragments; some of these are extensively developed producing stair-step features from one

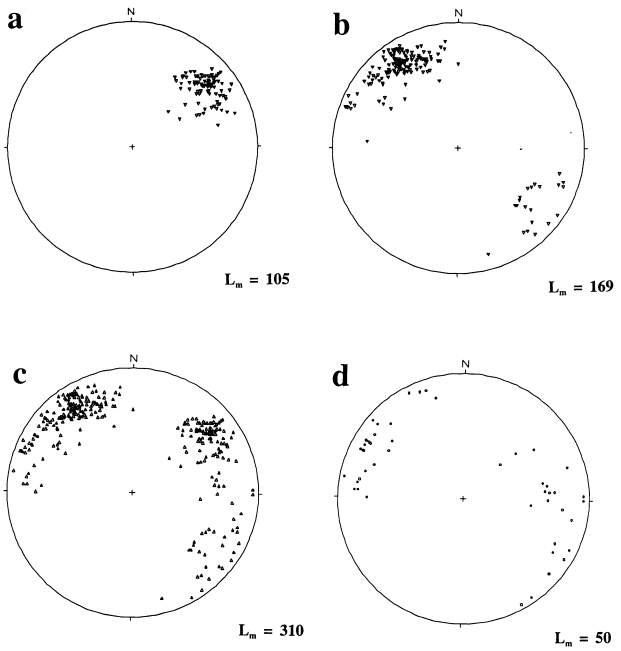

Fig. 12. Lower-hemisphere equal-area stereographic projections of structures in mylonitic rocks. (a) Stretching lineation (L_m) measured in mylonitic granite (Galeh–Doz pluton) and the mean orientation is 17°/052°. (b) Stretching lineation measured in mylonitic granite (west–northwest extension of the Galeh–Doz pluton) and the mean orientation is 15°/323°. (c) Stretching lineation measured in all mylonitic rocks of the study area. (d) Stretching lineation measured in amphibolite mylonite.

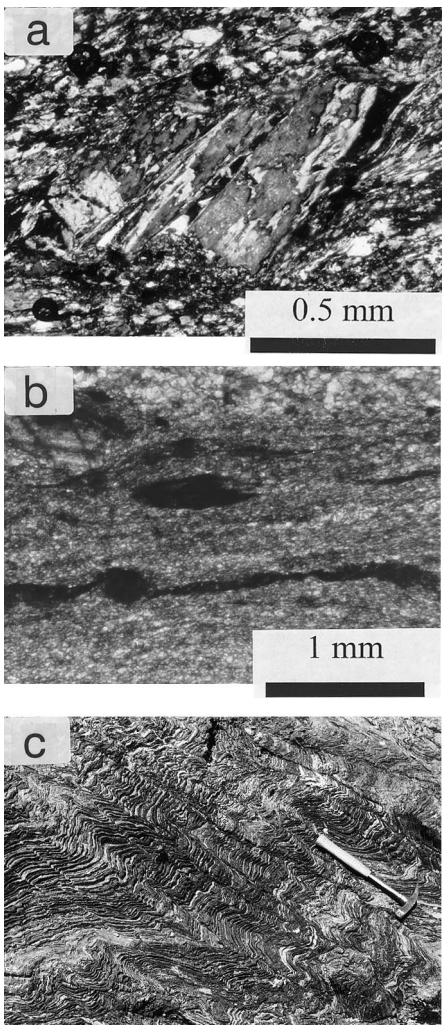

Fig. 13. (a) Antithetic shears in sheared greenschist with a hornblende porphyroclast internally broken by parallel fractures. Fragments of the porphyroclast are separated and sinistrally displaced due to dextral shear. Note that the chlorite fibres in fractures have grown subparallel to the *C*-plane. Sample number 472, crossed polarised light. (b) δ-type asymmetric porphyroclast of calcite developed by dextral shear in calcite mylonite. Sample number 32, plane polarised light. (c) S_3 in a thin-layered marble. Middle unit of the June Complex, 1 km southwest of Papion. Hammer is 32 cm in length.

grain to the next. Displaced broken grains are used for determining shear sense in mylonitic rocks (Simpson and Schmid, 1983; Takagi, 1986). Amphiboles that were unable to deform plastically have fractured with bookshelf type rotation in the amphibolite mylonite reflecting dextral shear (Fig. 13a).

5.3. Calcite mylonite

Calcite mylonite is well developed in some parts of the study area and is composed of very fine-grained calcite and recrystallised dolomite porphyroclasts. Porphyroclasts have wings of fine-grained dolomite and a strong foliation (S_2) is produced by the elongation and alignment of calcite minerals and by pressure solution as shown by concentration of graphite and insoluble residues along foliation planes. Hinges of microfolds are preserved as pods due to strong transposition along the mylonitic foliation. In a thin section cut parallel to stretching lineation and perpendicular to mylonitic foliation, δ-type asymmetric tails occur in the calcite mylonite and indicate dextral shear (Fig. 13b).

5.4. Mylonitic silicic igneous rocks

Along the northern border of the mylonitic granite, within the Hamadan Phyllite, fine-grained mylonitic silicic igneous rocks are exposed with a west-northwest trend. These rocks may have been fine-grained intrusions associated with the Galeh–Doz pluton. The mylonitic foliation (S_2) in this fine-grained silicic ultramylonite is parallel to the axial planes of tight to isoclinal F_2. A strong stretching lineation in S_2 is subhorizontal or gently plunging either to the west-northwest or to the east-southeast (Fig. 12).

6. D_3–D_4 deformations

Locally, weakly developed third and fourth deformations are recognised in the study area (Mohajjel, 1997). The third deformation is characterised by locally developed F_3 folds and S_3 crenulation cleavage (Fig. 13c). F_3 folds are upright, close to open in competent rocks and close in phyllite. Axial planes are mostly vertical or steeply dipping to the north-northeast and hinges are moderately plunging to the east-northeast. F_3 folds have low amplitudes and long wavelengths. S_3 is an axial planar crenulation cleavage and is vertical or dips steeply to the northeast. D_3 thrust faults are generally identified by cross-cutting relations with S_2 and are associated with brecciation. Two sets of steeply dipping strike-slip faults occur: the northeasterly trending faults (010–040°) are sinistral and the northwesterly trending faults (320–350°) are dextral. They are mostly developed in the northern limb of the map-scale F_2 and displace S_2 and D_2 thrust faults. A general north–south direction of shortening is indicated for these two fault sets and therefore they are considered as part of the third deformation event in the area.

In contrast to the previous deformations, the last deformation is recognised by northeast–southwest-trending folds, and conjugate dextral and sinistral kinks that are developed in schist and phyllite. F_4 are open, upright folds with axes plunging both to the northeast and southwest and lacking an axial plane cleavage. Within the study area dextral and sinistral kink bands occur in schist and phyllite and were produced by post D_3 foliation-parallel compression.

7. Discussion

D_1 structures have been obliterated or strongly reoriented by pervasive D_2. The variable trends of F_1 folds reflect the intensity of the D_2 deformation. The highest metamorphic grades associated with this deformation occur in the core of the major F_2 antiform near Baraftab–Deraz where amphibolite has hornblende and plagioclase defining the S_1 foliation and indicating peak metamorphism of amphibolite facies during the D_1 deformation (Mohajjel, 1997). The precise tectonic significance of the D_1 deformation is difficult to establish due to the intensity of D_2. D_1 may have formed as part of a continuum deformation with D_2. Alternatively, the D_1 deformation may have formed as a discrete tectonic episode. Northwest of the study area a regional angular unconformity, overlain by middle Cretaceous sedimentary and volcanic rocks, indicates general uplift in the Sanandaj–Sirjan Zone in the Late Jurassic–Early Cretaceous (Mohajjel, 1997). This tectonic event is thought to be related to subduction that occurred during Late Jurassic–Early Cretaceous times along the northeastern active continental margin of Neo-Tethys (e.g. Sengör et al., 1988) and may also account for the D_1 deformation and associated metamorphism (Mohajjel, 1997).

In contrast to the tectonic significance of the D_1 deformation, the tectonic significance of the D_2 deformation is well constrained. The D_2 deformation is recognised throughout much of the northwestern Sanandaj–Sirjan Zone and affects all Mesozoic metamorphic units including low-grade Cretaceous sedimentary and volcanic successions above the angular unconformity noted above (Mohajjel, 1997). In the later stages of deformation thrusts have cut the overturned southwestern limbs of the major F_2 antiforms and have transported these rocks to their present structural level during major uplift associated with D_2 transport to the south-southwest. In the study area, all rock units are affected by this deformation apart from

dolerite of presumed Tertiary age. The D_2 deformation is associated with the development of syntectonic biotite and actinolite indicating greenschist facies metamorphism (Mohajjel, 1997). D_2 deformation is constrained to the Late Cretaceous by a suite of post-tectonic Palaeocene plutons that are widely developed in the northwestern Sanandaj–Sirjan Zone (e.g. Valizadeh and Cantagrel, 1975). These constraints indicate that the D_2 deformation is the result of collision of the Afro-Arabian continent with the southwestern part of central Iran (Sanandaj–Sirjan Zone) which occurred in the Late Cretaceous (e.g. Alavi, 1994). The D_2 deformation is the product of dextral transpression (see below).

Locally observed F_3 folds are coaxial with F_2 folds and F_3 axial surfaces are co-planar with F_2 axial surfaces indicating that during D_3, the same shortening direction of both D_1 and D_2 was maintained. For D_4 shortening was almost perpendicular to the shortening direction of the previous deformations.

7.1. Deformation partitioning

Deformation partitioning has been reported at a

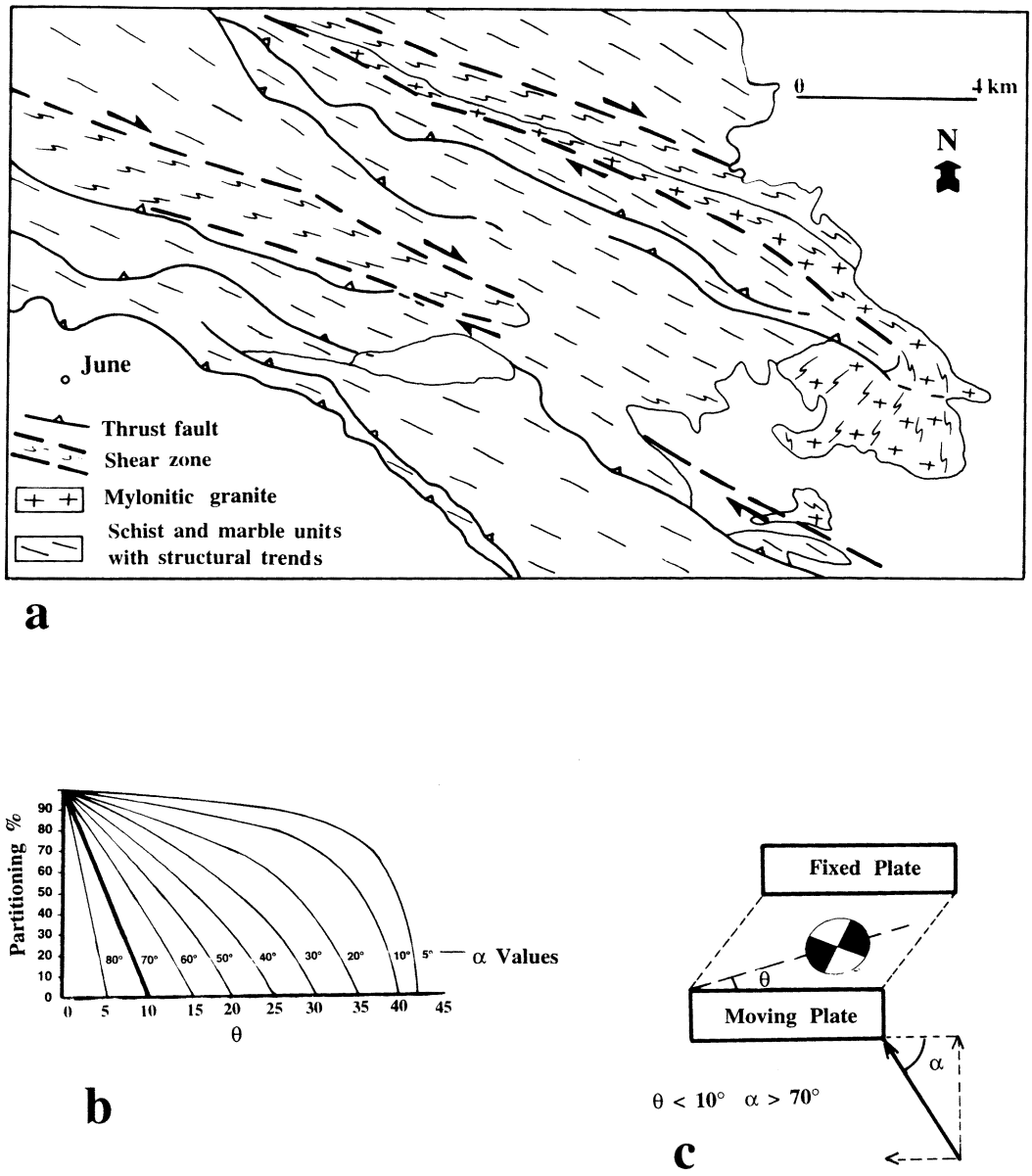

Fig. 14. (a) General structure map of the June area showing two domains of deformation partitioning: (1) schist and marble rock units, and (2) mylonitic rock units. (b) Graph showing the relationship between the angle of plate motion (α), the orientation of the instantaneous strain axes (θ) and the percentage of deformation partitioning (after Tikoff and Teyssier, 1994). For the June area $\alpha > 70^\circ$ and $\theta < 10^\circ$. (c) Model for partitioning in a pure-shear dominated zone of transpression ($\alpha > 70^\circ$ and $\theta < 10^\circ$) after Tikoff and Teyssier (1994).

macroscopic scale in polydeformed orogenic belts, with progressive localisation of strain during several deformation stages (e.g. Worley and Wilson, 1996), and in a single deformation event (Bergh and Karlstrom, 1992). Deformation partitioning in the study area has occurred on a macroscopic scale during D_2 and has formed two interleaved high-strain domains that are controlled by rock type (Fig. 14).

The domain with schist and marble units is strongly folded and foliated with axial plane S_2 schistosity regionally developed. In addition, thrusts have displaced units and indicate a north-northeast–south-southwest shortening direction that is consistent with the orientation of F_2 and S_2. The flattened shapes of the map-scale F_2 are consistent with a vertical stretching in this domain although this was not strong enough to develop a stretching lineation. Evidence for non-coaxial shearing is limited apart from occasional asymmetric boudins (e.g. Fig. 8b). In the absence of widespread criteria indicating non-coaxial shearing it is inferred that this domain was mainly affected by coaxial deformation.

The mylonitic rocks of the second domain are characterised by steeply dipping mylonitic foliation (S_2) and a west-northwesterly-trending subhorizontal stretching lineation in the mylonitic foliation. Dextral shearing is well illustrated by widespread shear-sense indicators. They indicate that D_2 had a major component of dextral shearing parallel to the west–northwest trend of the structural grain in the study area. The map-scale geometry of the syn-D_2 Galeh–Doz pluton is also interpreted as having formed during the episode of dextral shearing (see below).

7.2. Transpression

Transpression involves strike-slip shear accompanying horizontal shortening and vertical lengthening in the shear plane (Sanderson and Marchini, 1984; Dewey et al., 1998). Tikoff and Teyssier (1994) have applied their model of tectonic transpression to present-day zones of oblique plate convergence and have recognised pure-shear dominated transpression (e.g. Sumatra) and simple-shear dominated (e.g. California) transpression. A feature of transpression is the partitioning of deformation into domains of pure-shear dominated deformation and simple-shear dominated deformation. A high degree of strike-slip partitioning occurs in plate boundaries with highly oblique convergence (i.e. simple shear dominated deformation). This has occurred in California along the San Andreas Fault (where $\alpha = 5°$, α is the angle of oblique convergence); here, strike-slip shearing occurs solely along the fault and the diffuse zone of deformation either side of the fault is characterised by nearly normal pure-shear deformation (Teyssier et al., 1995).

In the present-day Zagros Mountains convergence is dextrally transpressive (Jackson, 1992) with $\alpha = 70°$, and a similar pattern is thought to have occurred during the Cretaceous collision (Mohajjel, 1997). In the study area, there has been strong partitioning between two domains as indicated by the development of mylonitic rocks dominated by dextral strike-slip shearing and another domain with far less evidence for non-coaxial shearing deformation in the schist and marble units. The shear zones in the mylonitic rocks are parallel to the plate margin along which the oblique convergence has occurred, but no strike-slip faults, parallel to the trend of the shear zones, have been observed (Mohajjel, 1997). This is unusual as generally partitioning of strike-slip shearing in transpressional zones occurs into strike-slip faults, even in regions with low obliquity (e.g. Sumatra, Tikoff and Teyssier, 1994). Thus the study area has been situated in a pure-shear dominated transpressional tectonic regime with a convergence direction at a high-angle to the plate margin.

This is somewhat similar to the deformation pattern recorded by Curtis (1997, 1998) in the Heritage Range

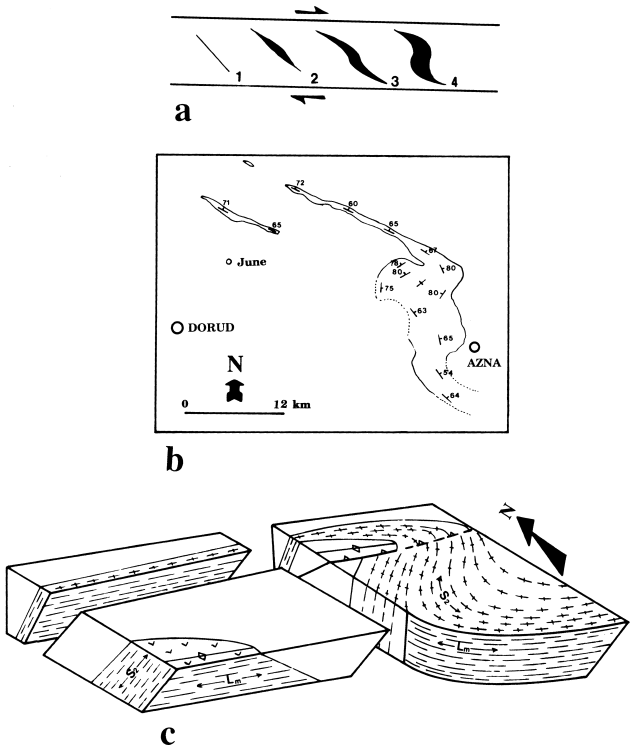

Fig. 15. Model for the emplacement of the Galeh–Doz pluton based on suggestion of Castro (1986) for Hercynian syntectonic granites in Spain. (a) Schematic en échelon extension fissures in a shear zone. Numbers indicate the stages of development. (b) Map of the Galeh–Doz pluton in the Dorud–Azna region. (c) Schematic block diagram shows the stretching lineation and mylonitic foliation in the mylonitic granite and amphibolite in the June area.

in West Antarctica where α was also equal to 70° (cf. Fig. 14). He recognised strong partitioning between two domains, one with reverse geometry (folds and thrusts), and one with dextral strike-slip shearing striking parallel to the regional structural grain. Overall, the region was affected by pure-shear dominated dextral transpression with efficient deformation partitioning in a zone with convergence at a high angle to the plate margin. From the theory devised by Tikoff and Teyssier (1994), the amount of partitioning between pure-shear dominated and simple-shear dominated domains is increased as the angle (θ) between the trend of the plate boundary and the maximum horizontal axis of the incremental strain ellipse is decreased. For the Heritage Range, with bulk-shear dominated transpression, where the percentage of partitioning is close to 100%, the angle θ will be very close to the zero. Curtis (1998) accounted for this by inferring that such efficient kinematic partitioning, not theoretically predicted or demonstrated by modern oblique convergent margins (Tikoff and Teyssier, 1994; Teyssier et al., 1995), was accommodated by pre-existing weak zones in the basement (see below).

7.3. Temporal and structural setting of the Galeh–Doz pluton

Paterson and Tobisch (1988) summarised the general characteristics of syntectonic plutons. These characteristics are all applicable to the Galeh–Doz pluton and listed below. (1) The strong steeply dipping foliation in the country rocks continues into the pluton with the same orientation. (2) The strong subhorizontal stretching lineation existing in the country rocks, such as mylonitic amphibolite and other mylonitic rocks, continues in the pluton. (3) Synkinematic contact metamorphism is associated with the Galeh–Doz pluton (see below). (4) The margin of the Galeh–Doz pluton is highly mylonitised. (5) The shape of the pluton is concordant with regional structure and it is extensively stretched along the strike of the foliation containing the subhorizontal stretching lineation.

Although the foliation has been dextrally rotated during shearing (see below), the consistency of the mylonitic foliation trajectories within the Galeh–Doz pluton demonstrates that no strain heterogeneities were produced due to pluton intrusion as described in some syntectonic plutons (e.g. Brun and Pons, 1981; Paterson et al., 1991). No pervasive magmatic foliation (Paterson et al., 1989), or a primary flow foliation formed from ballooning (Hutton, 1988), is recognised in the pluton because of the presence of the intense mylonitic foliation (S_2). Pluton boundaries are subparallel to the mylonitic S_2 and the pluton is elongate along the stretching direction (west-northwest).

To the southeast of Galeh–Doz, near the contact of the schist with deformed granite, a weak contact metamorphic effect is evident and defined by growth of muscovite and biotite in S_2. The same weak contact effect is observed along the west-northwest-trending extension of the Galeh–Doz pluton.

7.4. Tectonic model for emplacement of the Galeh–Doz pluton

A tectonic model for the emplacement of the Galeh–Doz pluton has to account for the pervasive dextral shearing and also the sigmoidal shape of the pluton. Emplacement of the Galeh–Doz pluton was syn-tectonic (see above) and therefore as it intruded it was deformed and extended in the west-northwest direction parallel to S_2 and the subhorizontal stretching lineation was developed throughout the pluton. Continuing dextral shearing caused rotation of the central part of the pluton as has been documented in en échelon sigmoidal gash veins (Ramsay and Huber, 1987, pp. 23–24, 48–52) and also in the syntectonic granites of the Hercynian belt of Spain (Castro, 1986). In the central part of the pluton, S_2 and L_m have been dextrally rotated (Figs. 3 and 12) producing a structure resembling the geometry of a δ-type porphyroclast (see Passchier and Simpson, 1986). Thus the dominant steeply dipping mylonitic S_2 of the northwestern extension of the pluton changes its strike through the main mass of the Galeh–Doz pluton (Fig. 14).

In the model of Castro (1986) the ascent and emplacement of syntectonic Hercynian granites was controlled by (1) development of a major cavity at 45° to the shear zone, (2) buoyancy-controlled magma intrusion along the cavity, and (3) rotation of the central part of the widening pluton (see Fig. 15). This model certainly accounts for the late history of the Galeh–Doz pluton (Fig. 15a, phases 3 and 4) but the extent of deformation precludes recognition of the early tensional-controlled phases.

Under the greenschist facies conditions endured during the D_2 deformation, some of the granitic rocks may be expected to have been more competent than rocks of the first domain. This is surprising given that non-coaxial deformation is normally focused into weaker units (e.g. Ridley, 1986), as is partially demonstrated in the study area by the development of calcite mylonite and retrogressed amphibolite. We see two solutions to this puzzle. Firstly, if the Galeh–Doz pluton intruded during the D_2 transpressive deformation then the cooling granite mass may have formed a weak zone that localised kinematic partitioning with enhancement of the non-coaxial shearing component (cf. Curtis, 1998, p. 304). Secondly, under upper greenschist facies conditions the Galeh–Doz granite may have been less competent than some of the surrounding schist–marble units reflecting difficulties in

judging competency under some metamorphic conditions (see Ramsay and Huber, 1987, pp. 397–401).

8. Conclusions

Several deformations occur in the study area in the Sanandaj–Sirjan Zone of western Iran. D_1 consists of east-dipping S_1 and F_1 plunging moderately to the east-northeast. D_2 is the major deformation with a strongly developed S_2 dipping steeply to the north-northeast and F_2 plunging moderately to the east. F_3 is locally developed and is coaxial with F_2.

The second deformation is related to oblique collision along the Sanandaj–Sirjan Zone in the Late Cretaceous. Deformation partitioning associated with dextral transpression during D_2 is reflected by the different responses of the rock units. Schist and marble units were intensely folded with southwest vergence and contain thrust faults that are subparallel to the trend of the S_2 and dipping to the north-northeast. In contrast, the syn-tectonic plutonic rocks, amphibolites and other mylonites have a regional S_2 foliation containing a subhorizontal west-northwest-trending stretching lineation and abundant dextral shear-sense criteria. The mylonitic foliation is sub-parallel to the regional S_2 schistosity in schist and marble units. In contrast to other regions affected by transpression, domains of non-coaxial deformation are developed in wide zones and not as weak narrow fault zones (e.g. Teyssier et al., 1995). The study area also illustrates the difficulty of judging competency of granitic rocks. These may have been deformed during cooling from high temperatures, and were therefore markedly more ductile than surrounding rocks. Alternatively, the competency of granitic rocks under upper greenschist facies conditions may be less than that commonly assumed.

Acknowledgements

M.M. acknowledges support from a scholarship provided by the Ministry of Culture and Higher Education, Islamic Republic of Iran. Field, laboratory and manuscript preparation was supported by research funds from the University of Wollongong. We thank Dave Carrie, Richard Miller and Penny Williamson for technical assistance. We gratefully acknowledge useful discussions with Professor Jim McLelland (Colgate University), Dr M. Alavi and Mr Reza Sahandi (Geological Survey of Iran). Helpful reviews by Christian Teyssier and in particular by an anonymous referee and Associate Editor Tom Blenkinsop substantially improved the final manuscript.

References

Alavi, M., 1994. Tectonics of the Zagros Orogenic belt of Iran: new data and interpretations. Tectonophysics 229, 211–238.

Berberian, M., King, G.C., 1981. Towards a palaeogeography and tectonics evolution of Iran. Canadian Journal of Earth Sciences 18, 210–265.

Bergh, S.G., Karlstrom, K.E., 1992. The Chaparral shear zone: deformation partitioning and heterogeneous bulk crustal shortening during Proterozoic orogeny in central Arizona. Geolgical Society of America Bulletin 104, 329–345.

Berthe, D., Choukroune, P., Jegouzo, P., 1979. Orthogneiss, mylonite and non coaxial deformation of granites: the example of the south Amorican Shear Zone. Journal of Structural Geology 1, 31–42.

Brun, J.P., Pons, J., 1981. Strain pattern of pluton emplacement in a crust undergoing non-coaxial deformation, Sierra Morena, Southern Spain. Journal of Structural Geology 3, 219–229.

Castro, A., 1986. Structural pattern ascent model in the Central Extremadura batholith, Hercynian belt, Spain. Journal of Structural Geology 8, 633–645.

Curtis, M.L., 1997. Gondwanian age dextral transpression and spatial kinematic partitioning within the Heritage Range, Ellsworth Mountains, West Antarctica. Tectonics 16, 172–181.

Curtis, M.L., 1998. Development of kinematic partitioning within pure-shear dominated dextral transpression zone: the southern Ellsworth Mountains, Antarctica. In: Holdsworth, R.E., Strachan, R.E., Dewey, J.F. (Eds.), Continental Transpressional and Transtensional Tectonics. Geological Society of London Special Publication 135, pp. 289–306.

Dewey, J.F., Holdsworth, R.E., Strachan, R.A., 1998. Transpression and transtension zones. In: Holdsworth, R.E., Strachan, R.E., Dewey, J.F. (Eds.), Continental Transpressional and Transtensional Tectonics. Geological Society of London Special Publication 135, pp. 1–14.

Hutton, D.H.W., 1988. Granite emplacement mechanisms and tectonic controls: inferences from deformation studies. Transactions of the Royal Society of Edinburgh: Earth Sciences 79, 245–255.

Jackson, J.A., 1992. Partitioning of strike-slip and convergent motion between Eurasia and Arabia in eastern Turkey and the Caucasus. Journal of Geophysical Research 97, 12471–12479.

Lister, G.S., Snoke, A.W., 1984. *S–C* mylonites. Journal of Structural Geology 6, 617–638.

Masoudy, F., 1997. Contact metamorphism and pegmatite development in the region SW of Arak, Iran. Ph.D. thesis, University of Leeds, UK (unpublished).

Mohajjel, M., 1997. Structure and tectonic evolution of Palaeozoic–Mesozoic rocks, Sanandaj–Sirjan Zone, western Iran. Ph.D. thesis, University of Wollongong, Wollongong, Australia (unpublished).

Passchier, C.W., Simpson, C., 1986. Porphyroclast systems as kinematic indicators. Journal of Structural Geology 8, 831–843.

Paterson, S.R., Vernon, R.H., Tobisch, O.T., 1989. A review criteria for determining magmatic and solid-state foliations in granitoids. Journal of Structural Geology 11, 349–363.

Paterson, S.R., Brudos, T., Fowler, K., Carlson, C., Bishop, K., Vernon, R.H., 1991. Papoose Flat pluton: forceful expansion or postemplacement deformation? Geology 19, 324–327.

Paterson, S.R., Tobisch, O.T., 1988. Using pluton ages to date regional deformations: problems with commonly used criteria. Geology 16, 1108–1111.

Ramsay, J.G., 1967. Folding and Fracturing of Rocks. McGraw-Hill, NewYork.

Ramsay, J.G., Huber, M.I., 1987. In: The Techniques of Modern Structural Geology. Volume 2 Folds and Fractures. Academic Press, London.

Ridley, J., 1986. Parallel stretching lineations and fold axes oblique to a shear displacement direction—a model and observations. Journal of Structural Geology 8, 647–653.

Sanderson, D.J., Marchini, W.R.D., 1984. Transpression. Journal of Structural Geology 6, 449–454.

Sengör, A.M.C., Altmer, D., Cin, A., Ustaomer, T., Hsu, K.J., 1988. Origin and assembly of the Tethyside orogenic collage at the expense of Gondwana Land. In: Audley-Charles, M.G., Hallam, A. (Eds.), Gondwana and Tethys. Geological Society of London, Special Publication 37, pp. 119–181.

Simpson, C., Schmid, S.M., 1983. An evaluation of criteria to deduce the sense of movement in sheared rocks. Geological Society of America Bulletin 94, 1281–1288.

Takagi, H., 1986. Implications of mylonitic microstructures for the geotectonic evolution of the Median Tectonic Line, central Japan. Journal of Structural Geology 8, 3–14.

Teyssier, C., Tikoff, B., Markley, M., 1995. Oblique plate motion and continental tectonics. Geology 23, 447–450.

Tikoff, B., Teyssier, C., 1994. Strain modelling of displacement-field partitioning in transpressional orogens. Journal of Structural Geology 16, 1575–1588.

Valizadeh, M.V., 1992. Experimental petrology and regional tectonics (andesites and granites). University of Tehran Publication Number 2131, Tehran (in Farsi).

Valizadeh, M.V., Cantagrel, J.M., 1975. Prèmieres données radiométricques (K–Ar et Rb–Sr) sur les micas du complexe magmatique du Mont Alvand, Près Hamadan (Iran occidental). Comptes Rendus, Academie des Sciences Paris, Série D 281, 1083–1086.

White, S.H., Burrows, S.E., Carreras, J., Shaw, N.D., Humphreys, F.J., 1980. On mylonites in ductile shear zones. Journal of Structural Geology 2, 175–187.

Worley, B.A., Wilson, C.J.L., 1996. Deformation partitioning and foliation reactivation during transpressional orogenesis, an example from the Central Longmen Shan, China. Journal of Structural Geology 18, 395–411.